Biosensors and Bioelectronics 31 (2012) 144–150

Contents lists available at SciVerse ScienceDirect

Biosensors and Bioelectronics

journal homepage: www.elsevier.com/locate/bios

An electrochemical sulfite biosensor based on gold coated magnetic nanoparticles modified gold electrode

Rachna Rawal, Sheetal Chawla, Chandra Shekhar Pundir*

Department of Biochemistry, M D University, Rohtak 124001, Haryana, India

ARTICLE INFO

Article history:
Received 8 August 2011
Received in revised form
21 September 2011
Accepted 6 October 2011
Available online 12 October 2011

Keywords:
Sulfite
Sulfite oxidase
Sulfite biosensor
Amperometric
Gold coated magnetic
Nanoparticles
Red and white wines

ABSTRACT

A sulfite oxidase (SO_X) (EC 1.8.3.1) purified from *Syzygium cumini* leaves was immobilized onto carboxylated gold coated magnetic nanoparticles (Fe_3O_4@GNPs) electrodeposited onto the surface of a gold (Au) electrode through N-ethyl-N′-(3-dimethylaminopropyl) carbodiimide (EDC)-N-hydroxy succinimide (NHS) chemistry. An amperometric sulfite biosensor was fabricated using SO_X/Fe_3O_4@GNPs/Au electrode as working electrode, Ag/AgCl as standard and Pt wire as auxiliary electrode. The working electrode was characterized by Fourier Transform Infrared (FTIR) Spectroscopy, Cyclic Voltammetry (CV), Scanning Electron Microscopy (SEM) and Electrochemical Impedance Spectroscopy (EIS) before and after immobilization of SO_X. The biosensor showed optimum response within 2 s when operated at 0.2 V (vs. Ag/AgCl) in 0.1 M Tris–HCl buffer, pH 8.5 and at 35 °C. Linear range and detection limit were 0.50–1000 μM and 0.15 μM (S/N = 3) respectively. Biosensor was evaluated with 96.46% recovery of added sulfite in red wine and 1.7% and 3.3% within and between batch coefficients of variation respectively. Biosensor measured sulfite level in red and white wines. There was good correlation (r = 0.99) between red wines sulfite value by standard DTNB (5,5′-dithio-bis-(2-nitrobenzoic acid)) method and the present method. Enzyme electrode was used 300 times over a period of 4 months, when stored at 4 °C. Biosensor has advantages over earlier biosensors that it has excellent electrocatalysis towards sulfite, lower detection limit, higher storage stability and no interference by ascorbate, cysteine, fructose and ethanol.

1. Introduction

Determination of sulfite is important from biological and industrial perspectives (Safavi and Ramezani, 1997). Sulfite is widely used as additive in food, beverages and pharmaceuticals to prevent oxidation and bacterial growth and control of enzymatic reactions during their production and storage. Sulfite is known to cause some cytotoxic, mutagenic and antinutritional effects (Stammati et al., 1992). It also interacts with some vitamins, i.e. pyridoxal, nicotinamide, thiamine, folic acid leading to reduced nutritional quality of treated food (Pizzoferrato et al., 1989). Sulfite oxidase (SO_X) occurs in the mitochondria of all eukaryotes. It oxidizes sulfite to sulfate and transfers the electrons produced, to the electron transport chain via cytochrome c, allowing generation of ATP in oxidative phosphorylation. Lack of functional SO_X causes a sulfite deficiency, which leads to neurological disorders, mental retardation, physical deformities, dislocated lenses, degradation of brain and early death. Thus sulfite level in the body must be maintained tightly. Normally, human serum has sulfite concentration in the range of 0–10 μM. Food and Drug Administration (FDA) has recommended warning labels on any food containing more than 10 mg/Kg or beverage containing more than 10 mg/L of sulfite (Dinckaya et al., 2007). Various techniques for quantitative determination of sulfite in different types of samples are available such as iodimetry, spectrophotometry, anodic stripping voltammetry, reciprocal oscillographic chronopotentiometry, ion chromatography, enthalpimetry, chemiluminescene, gravimetry, gas chromatography, fluorometry and HPLC (Kaeil et al., 1989; Sezginturk and Dinckaya, 2005; Theisen et al., 2010). However, some of these methods lack sensitivity and precision (e.g. iodimetry, spectrophotometry), while others require time consuming sample preparation, expensive equipments and skilled person to operate. It is therefore, of considerable interest to develop a biosensing method for the detection of sulfite, as it would allow fast, selective and accurate determination of sulfite without the need of sample pretreatment and expensive equipment. A number of sulfite biosensors have been reported based on glassy carbon electrode coated with thin mercury film (Dinckaya et al., 2007), polypyrrole films (Ameer and Adeloju, 2008), polyaniline-sulfonic acid layer (Spricigo et al., 2009) and polyaniline film (Bahmani et al., 2010). However, these biosensors suffer from restricted detection limit due to poor electron flow and lower storage stability of the enzyme electrode.

Currently, nano-magnetic particles are attracting more attention due to their distinguished properties, such as small scale effect,

* Corresponding author. Mobile: +91 9416492413.
E-mail addresses: pundircs@rediffmail.com, pundircs@gmail.com (C.S. Pundir).

0956-5663/$ – see front matter © 2011 Elsevier B.V. All rights reserved.
doi:10.1016/j.bios.2011.10.007

surface effect, special magnetic target and good biocompatibity properties (Zhu et al., 2006; Laurent et al., 2008; Zhang et al., 2008). Among a variety of metal oxide nanoparticles, Fe_3O_4 nanoparticles are particularly attractive due to their magnetic and electrical properties (Wan et al., 2007). Nano-sized magnetic bioconjugated materials have been used in electrochemical biosensors due to their many unique properties such as large surface area, higher bioactivity, excellent conformation stability and better contact between biocatalyst and its substrate (Katz et al., 2004; Li, 2007; Jaffrezic-Renault et al., 2007). The magnetic properties are influenced by surface effects. Hence, a more robust structure for nanoparticles is a shell configuration, where the magnetic core is coated by a shell layer (Bodker et al., 1994). Additionally, the shell provides a platform for surface modification, functionalization, tuning magnetic properties and biocompatibility (Cho et al., 2005). The synthesis of gold coated iron nanoparticles (Fe_3O_4@GNPs) is of special interest, since gold coating results into the formation of air-stable nanoparticles, which are protected from oxidation. Surface derivatization with gold also helps to reduce particle agglomeration by steric or electronic repulsion and improves biocompatibility (Daniel and Astruc, 2004).

Thus, the present work was aimed to construct an amperometric sulfite biosensor based on covalent binding of SO_X onto gold coated magnetic nanoparticles (Fe_3O_4@GNPs), using N-ethyl-N-(3-dimethylaminopropyl) carbodiimide (EDC) and N-hydroxy succinimide (NHS) chemistry and employ it for measurement of sulfite level in red and white wines.

2. Materials and methods

2.1. Reagents

Sephadex G-100, DEAE-Sephacel from Sigma–Aldrich, St. Louis, USA. N-Ethyl-N-(3-dimethylaminopropyl) carbodiimide (EDC), N-hydroxysuccinimide (NHS), Folin-Ciocalteu's phenol reagent from SISCO Research Laboratory were used. All other chemicals were of analytical reagent (AR) grade. Different brands of red and white wines were purchased from market of different states of India. Double distilled water (DW) was used throughout the experiments.

2.2. Apparatus

All electrochemical experiments were performed on an Autolab PGSTAT 30 electrochemical workstation (Eco Chemie BV, The Netherlands) with the GPES 4.9 software. A modified Au electrode of 1.0 mm diameter, a KCl-saturated Ag/AgCl electrode and a Pt electrode served as the working, reference, and counter electrodes respectively, in all electrochemical experiments. All potentials were measured with respect to the reference electrode. All experiments were done at room temperature. Scanning electron microscopic (SEM) images were taken in a Scanning Electron Microscope (Make: Model Joel JSM-6510, Japan) at Advanced Instrumentation Research Facility, JNU, New Delhi. Fourier Transform Infrared (FTIR) Spectroscopy was performed on FTIR spectrometer (Model iS10, Thermoelectron, USA).

2.3. Extraction and purification of SO_X from leaves of Syzygium cumini (Jamun)

SO_X from frozen jamun leaves was extracted as described (Ahmad and Sarfraz, 2010) with modification by homogenizing leaves with cold 0.1 M Tris–HCl (pH 8) in 3:1 ratio (w/v) in a chilled pestle and mortar. The extract was filtered through a muslin cloth and the filtrate was centrifuged at 10,000 × *g* for 30 min at 4 °C. The pellet was discarded and supernatant was collected and treated as crude enzyme. It was tested for sulfite oxidase activity and protein concentration by Lowry method. Crude enzyme was purified as described (Satyapal and Pundir, 1993) using a combination of 0–80% ammonium sulfate precipitation, gel filtration on Sephadex G-100 and ion-exchange chromatography on DEAE-Sephacel using linear gradient of KCl (0.1–0.6 M). Finally, the enzyme was purified by 57-fold with 19.5% yield.

2.4. Assay of SO_X

The assay of SO_X was carried out as described (Satyapal and Pundir, 1993) with modifications and based on quantification of H_2O_2 generated from sulfite, using a color reaction consisting of 4-aminophenazone, phenol and peroxidase as chromogenic system. The reaction mixture containing 1.8 mL of 0.1 M Tris–HCl buffer pH 8.5, and 0.1 mL enzyme preparation was preincubated at 35 °C for 5 min. The reaction was started by adding 0.1 mL of 0.4 mM sodium sulfite. After incubation at 35 °C for 10 min in dark, 1.0 mL color reagent was added and kept at room temperature for 15 min to develop the color. A_{520} was read and H_2O_2 content generated during the reaction was interpolated from a standard curve between H_2O_2 conc. and A_{520} prepared in 0.1 M Tris–HCl buffer, pH 8.5.

One unit of enzyme is defined as amount of enzyme required to catalyze the formation of 1.0 nmole of H_2O_2 from oxidation of sulfite per min under standard assay conditions.

2.4.1. Preparation of color reagent

The color reagent was prepared as described (Bias et al., 1980) and consisted of 50 mg 4-aminophenazone, 100 mg solid phenol and 1 mg horseradish peroxidase per 100 mL of 0.4 M sodium phosphate buffer, pH 7.0. It was stored in amber colored bottle at 4 °C and discarded after one week.

2.5. Preparation of gold coated magnetic nanoparticles (Fe_3O_4@GNPs)

Firstly, Fe_3O_4 magnetic nanoparticles were prepared as described (Kuang et al., 2002). Before mixing, 0.4 M hydrochloric acid and 0.7 M ammonia solution were bubbled by nitrogen for 10 min $FeCl_3{\cdot}6H_2O$ (8.5 g) and $FeCl_2{\cdot}4H_2O$ (3.0 g) were dissolved in 38 mL of 0.4 M hydrochloric acid, then added quickly to 375 mL 0.7 M ammonia solution under vigorous stirring (non-magnetic) at room temperature. After half-an-hour stirring, the precipitates were isolated by magnetic force. The precipitates were washed thoroughly with DW. Then, the reduction of Au^{3+} onto the surface of magnetic nanoparticles was carried out in ethanol, to modify them with GNPs. To achieve it, magnetic nanoparticles were dispersed into 100 mL of 1 mM $HAuCl_4$ (chloroauric acid) solution and mixed with 10 mL of an ethanol (10 mg/mL). The resulting mixture was allowed to stand for 15 min at room temperature, and then the prepared magnetic-gold nanoparticles were separated from colloid by a magnet. Finally, the nanoparticles were washed three times with DW. The characterization of Fe_3O_4 NPs and Fe_3O_4@GNPs was carried out by Transmission Electron Microscopy (TEM).

2.6. Carboxylation of Fe_3O_4@GNPs

The carboxyl groups were introduced onto Fe_3O_4@GNPs nanoparticles (1.5 g) surface by immersing the nanoparticles into 15 mL of 20 mM ethanolic solution of 3-mercaptopropionic acid (3-MPA) and kept for 48 h to allow binding of 3-MPA molecules onto the surface of Fe_3O_4@GNPs nanoparticles via the well known thiol chemistry. Then the modified magnetic nanoparticles were rinsed in DW and dried in a vacuum oven for 6 h (Mikhaylova et al., 2004).

2.7. Electrodeposition of Fe_3O_4@GNPs onto Au electrode

Prior to the surface modification, the Au electrode was cleaned with piranha solution [H_2SO_4:H_2O_2 in ratio 3:1 (v/v)] for 20 min and then rinsed thoroughly with DW. The electrode was polished with alumina slurry. Fe_3O_4@GNPs were electrochemically deposited onto Au electrode through cyclic voltammetry (CV) by immersing Au electrode into a solution (25 mL) containing 22 mL electrolyte [2.5 mM $K_3Fe(CN)_6$/$K_4Fe(CN)_6$ (1:1)] and 3 mL carboxylated Fe_3O_4@GNPs and applying 30 polymerization cycles at −0.4 to +0.6 V (vs. Ag/AgCl) at a scan rate of 50 mV s^{-1}. The resulting Fe_3O_4@GNPs/Au modified electrode was washed thoroughly with DW to remove unbound matter and kept in dry petri plate at 4 °C.

2.8. Immobilization of SO_X on Fe_3O_4@GNPs/Au electrode

SO_X was immobilized onto carboxylated Fe_3O_4@GNPs/Au electrode by EDC–NHS chemistry (Rahman et al., 2009). Firstly, Fe_3O_4@GNPs modified Au electrode was immersed into 0.1 M phosphate buffer (pH 7.5) containing EDC and NHS of same concentration (10 mM) for 6 h and then excess of EDC and NHS were removed by washing with 0.1 M sodium phosphate buffer (PB) (pH 7.5). Finally, EDC–NHS activated electrode was immersed into 5 mL 0.1 M PB, pH 7.5 containing 100 μL enzyme solution (containing 3.0 μg protein) and kept overnight at 4 °C and thereafter taken off from PB and washed with DW.

2.9. Characterization of enzyme electrode

The modified Au electrode, at different stages of its construction was characterized using SEM, Fourier transform infrared spectroscopy (FTIR) and Electrochemical Impedance Spectroscopy (EIS) techniques. FTIR spectroscopy was performed to study the binding of SO_X with Fe_3O_4@GNPs composite film. The EIS measurements were carried out in 1 mM $K_3[Fe(CN)_6]$ in the 0.1 M PBS pH 7.0 at ambient temperature, at the polarization potential of 0.2 V (vs. Ag/AgCl) in the frequency range 0.1–10^4 Hz and with the amplitude of 10 mV.

2.10. Response measurement of SO_X/Fe_3O_4@GNPs/Au electrode

Cyclic voltammetric measurements were carried out in a three electrode cell containing 15 mL Tris–HCl buffer (0.1 M, pH 8.5). The reaction was started by adding 0.1 mL of sulfite (0.4 mM). Current (μA) was measured applying CV in the potential range between −0.4 and +0.6 V (vs. Ag/AgCl). The optimum current was obtained at 0.2 V (vs. Ag/AgCl), hence the subsequent electrochemical studies were carried out at this potential.

2.11. Optimization of SO_X/Fe_3O_4@GNPs/Au electrode

To determine the optimum working conditions of the enzyme electrode, the pH of reaction buffer (0.1 M) was varied from pH 5.0 to 9.5 at an interval of pH 0.5 using sodium phosphate buffer between pH 5.0 and 7.0 and Tris–HCl buffer between pH 7.5 and 9.5. Similarly, to determine optimum temperature, the reaction mixture was incubated at 15–55 °C at an interval of 5 °C. Optimum response time was studied by measuring current between 0 and 12 s at an interval of 3 s. To study the effect of substrate concentration, different sulfite concentration were used, in the range from 0.50 μM to 1000 μM. Apparent K_m and I_{max} for sulfite were calculated from Lineweaver–Burk plot based on the following equation:

$$\frac{1}{I} = \frac{K_m}{I_{max}}\frac{1}{[S]} + \frac{1}{I_{max}}$$

where K_m = Michaelis–Menten constant, I_{max} = maximum current and S = sulfite concentration

The amperometric response was also measured in the presence of potential interfering compounds found in real samples such as glucose, fructose, ascorbic acid, cysteine, acetic acid, ethanol and citric acid at their physiological concentration.

2.12. Evaluation

The following criteria was studied to evaluate the analytic performance of the biosensor, e.g. linearity, analytical recovery, detection limit, precision and correlation. Analytical recovery was studied using red wines with two different standard concentrations (50 and 100 μM) of sulfite. To test the reproducibility and reliability of the present biosensor, sulfite level in six red wine samples was measured five times on single day (within batch) and five times again after their storage at −20 °C for one week (between batch). To study the correlation the sulfite level was measured in 15 brands of red wine by the standard (5,5′-dithio-bis-(2-nitrobenzoic acid)) (DTNB) method and the present method and their correlation was studied by using regression equation.

To examine the long-term storage stability, the activity of enzyme electrode was tested upto 4 months at an interval of 1 week, when stored at 4 °C. To reuse the enzyme electrode, it was washed 3–4 times with reaction buffer before its use in next assay.

2.13. Amperometric measurement of sulfite in red and white wines

Sulfite level in red and white wine samples was measured by the present biosensor in the same manner as described above for its response measurement under its optimal working conditions except that sulfite was replaced by the sample. The current (μA) was recorded and the amount of sulfite was interpolated from standard curve between sulfite concentrations and current (μA) prepared under optimal working conditions.

3. Results and discussion

3.1. TEM study of Fe_3O_4 and Fe_3O_4@GNPs

TEM images of Fe_3O_4NPs demonstrated their good crystallinity and uniform distribution of size between 20 and 100 nm (Supplementary Fig. 1A), while Fe_3O_4@GNPs showed little aggregation, with grouping of the particles (size 100–120 nm) (Supplementary Fig. 1B).

3.2. Construction of modified enzyme electrode

A method is described for construction of a SO_X/Fe_3O_4@GNPs/Au electrode. Scheme 1 summarizes the different chemical reactions involved in the fabrication of SO_X electrode based on covalent immobilization of SO_X onto Fe_3O_4@GNPs/Au electrode through amide bond formation between the free –COOH groups of carboxylated Fe_3O_4@GNPs/Au electrode and free –NH_2 groups on surface of enzyme.

3.3. Response measurements of SO_X/Fe_3O_4@GNPs/Au electrode

Fig. 1 shows cyclic voltammograms of electrochemical deposition of Fe_3O_4@GNPs on the surface of Au electrode in a solution of 2.5 mM $K_3Fe(CN)_6$/$K_4Fe(CN)_6$ and PB 0.1 M (pH 7.5). No peak was observed for bare Au electrode (curve a) in PB. The cyclic voltammogram of Fe_3O_4@GNPs identified an oxidation peak at +125 mV (vs. Ag/AgCl) (curve b), and the modified SO_X/Fe_3O_4@GNPs/Au

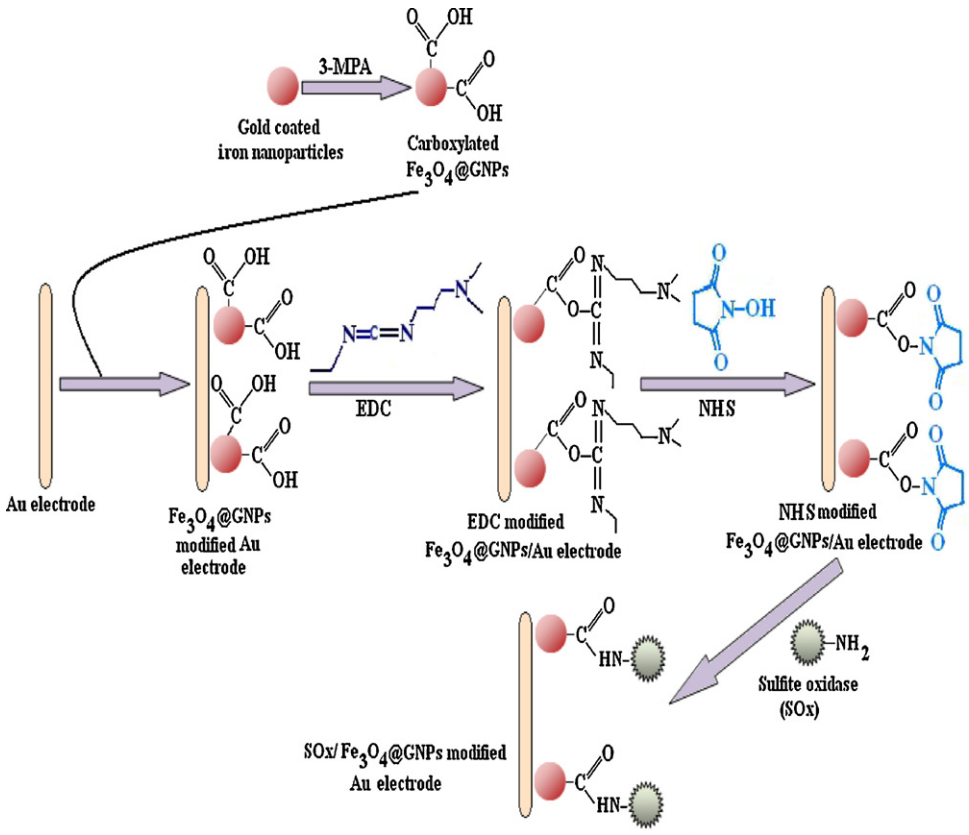

Scheme 1. Schematic representation of chemical reactions involved in fabrication of SO_X/Fe_3O_4@GNPs/Au electrode.

electrode also showed an oxidation peak at +200 mV (vs. Ag/AgCl) (curve c). The oxidation and reduction peaks of curve b correspond to the enhancement of peak current of Au electrode, after electrodeposition of Fe_3O_4@GNPs. The increase in peak current of curve c was due to oxidation of sulfate, hydrolysis product of sulfite, catalyzed by immobilized SO_X. This well defined oxidation peak [at 200 mV (vs. Ag/AgCl)] clearly indicates the catalytic properties of modified electrode.

The following electrochemical reactions involved in the response measurement of present amperometric sulfite biosensor:

$$\text{Sulfite} + O_2 + H_2O \xrightarrow{SO_X} \text{Sulfate} + H_2O_2$$

$$H_2O_2 \xrightarrow{0.2\,V} 2H^+ + O_2 + 2e^-$$

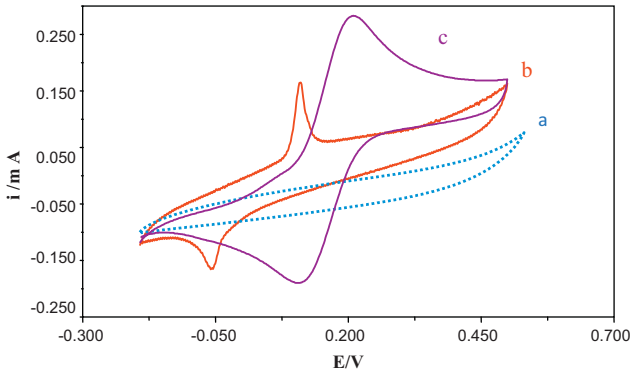

Fig. 1. Cyclic voltammograms (CVs) of (a) bare Au electrode, (b) Fe_3O_4@GNPs/Au electrode and (c) SO_X/Fe_3O_4@GNPs/Au electrode.

$$2e^- \xrightarrow{Fe_3O4@GNPs} \text{Au electrode}$$

3.4. Surface characterization by SEM

The surface morphologies of bare Au electrode, Fe_3O_4@GNPs/Au electrode and SO_X/Fe_3O_4@GNPs/Au electrodes were studied by SEM (Supplementary Fig. 2) Bare electrode showed homogenous surface (Supplementary Fig. 2A), whereas Fe_3O_4@GNPs/Au electrode has uniform granular porous morphology attributed to the homogeneous dispersion of GNPs in Fe_3O_4 nanoparticles (Supplementary Fig. 2B). The granular structural morphology of Fe_3O_4@GNPs was changed into the aggregated form in SO_X/Fe_3O_4@GNPs/Au, due to covalent immobilization of SO_X between enzyme molecule and carboxylated Fe_3O_4@GNPs (Supplementary Fig. 2C).

3.5. FTIR spectra

Fig. 2A displays the FTIR spectra of pure Fe_3O_4 nanoparticles (curve a), which exhibit strong absorption bands in the low frequency region 800 cm^{-1}, due to the iron nanoparticle skeleton. Other prominent bands at 617 and 582 cm^{-1} belong to the stretching vibration mode and the torsional vibration mode of Fe–O bonds in the tetrahedral sites and in the octahedral sites of Fe_3O_4 nanoparticles. FTIR spectra of Fe_3O_4@GNPs/Au electrode in the KBr matrix exhibited a strong characteristic absorption bands at 3380 cm^{-1} (H–O stretching), 1626 cm^{-1} (H–O–H bonding) (curve b), which were due to adsorbed water on the surface of nanoparticles. The absorption bands at 628 and 566 cm^{-1} of composites in curve b were weak, which resulted from the fact that the nanogold hindered the infrared absorption of Fe_3O_4. FTIR spectra of

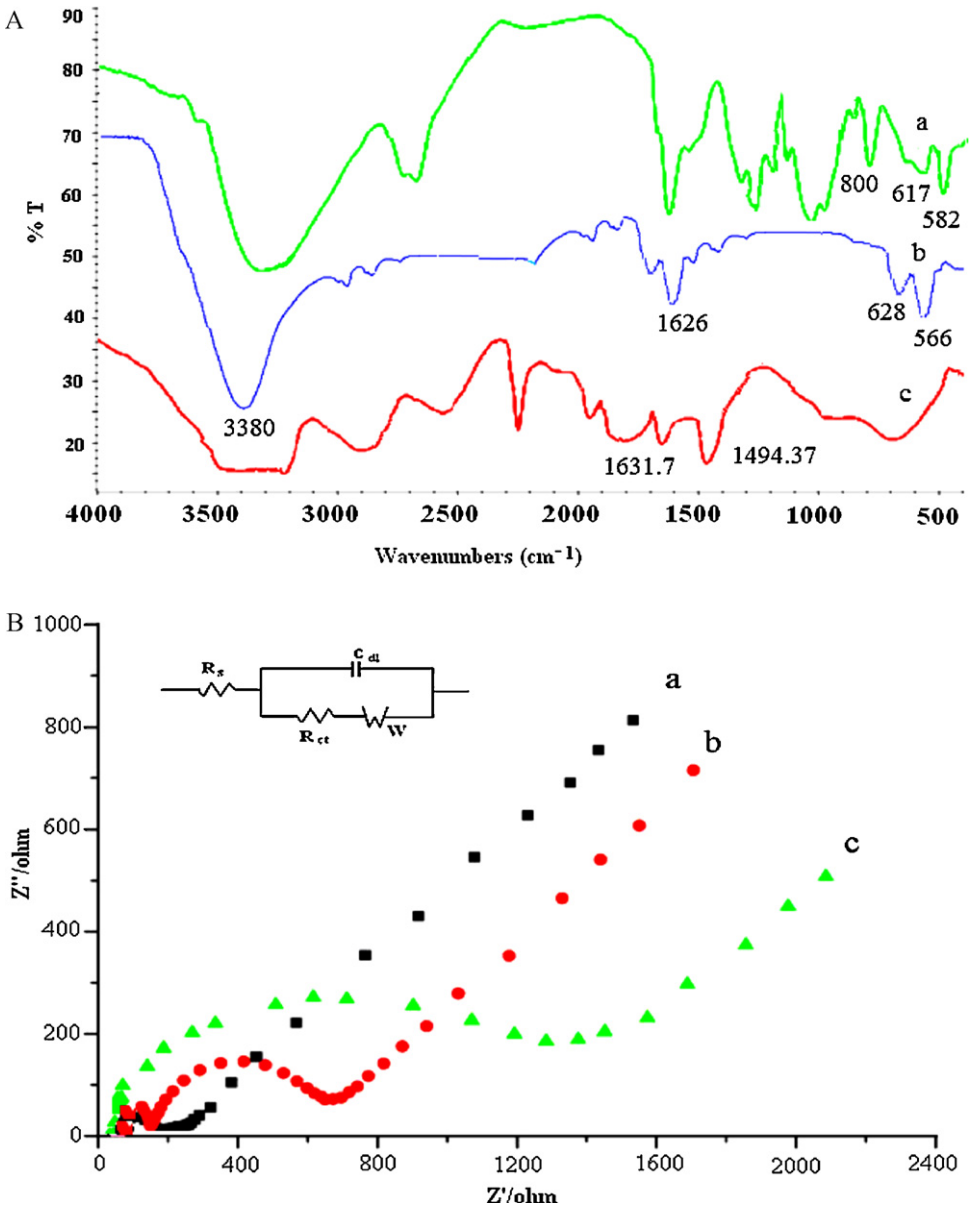

Fig. 2. (A) FTIR transmission spectra (a) Fe_3O_4 nanoparticles, (b) Fe_3O_4@GNPs nanoparticles and (c) SO_X/Fe_3O_4@GNPs nanoparticles. (B) Impedance spectra of (a) bare Au electrode, (b) Fe_3O_4@GNPs/Au electrode and (c) SO_X/Fe_3O_4@GNPs/Au electrode.

SO_X/Fe_3O_4@GNPs/Au (curve c) exhibited bands at 1631.70 and 1494.37 cm^{-1} assigned to the carbonyl stretch (amide I band) and –N–H (amide II band) respectively showing the covalent immobilization of SO_X.

3.6. Electrochemical Impedance measurements

Fig. 2B shows EIS of (a) bare Au electrode, (b) Fe_3O_4@GNPs/Au electrode and (c) SO_X/Fe_3O_4@GNPs/Au electrode respectively. EIS analysis was employed to investigate the change in charge transfer after immobilization of SO_X onto Fe_3O_4@GNPs/Au electrode. The value of the charge transfer resistance (semicircle diameter) (R_{CT}) depends on the dielectric and insulating features at the electrode/electrolyte interface. In EIS, the bare electrode exhibited an almost straight line (curve a), which is characteristic of a diffusional limiting step of the electrochemical process. The value of R_{CT} was 700 Ω for Fe_3O_4@GNPs electrode (curve b) and then increases to 1400 Ω for SO_X/Fe_3O_4@GNPs/Au electrode (curve c). The increased R_{CT} value of SO_X/Fe_3O_4@GNPs/Au electrode is attributed to the fact that most biological molecules, including enzymes are poor electrical conductors at low frequencies and cause hindrance to the electron transfer. These results confirm the successful assembly of the enzyme electrode.

3.7. Optimization of the biosensor (SO_X/Fe_3O_4@GNPs/Au electrode)

The biosensor showed optimum response (current in μA) at pH 8.5, which is higher than that for SO_X bound to screen printed strip modified carbon electrode (pH 7.5) (Abass et al., 2000), glassy carbon coated thin mercury film (pH 7.0) (Dinckaya et al., 2007), polypyrrole film (pH 7.0) (Ameer and Adeloju, 2008), but comparable to that of SO_X bound to polyaniline on aluminium surface (8.5) (Mohammad, 2008). Therefore, a pH of 8.5 was used in further experiments. The optimum temperature of biosensor was 35 °C, which is lower than that for glassy carbon coated thin mercury film (40 °C) (Dinckaya et al., 2007). The effect of the scan rate from 10 to 100 mV s^{-1} on the biosensor response using 0.4 mM sodium

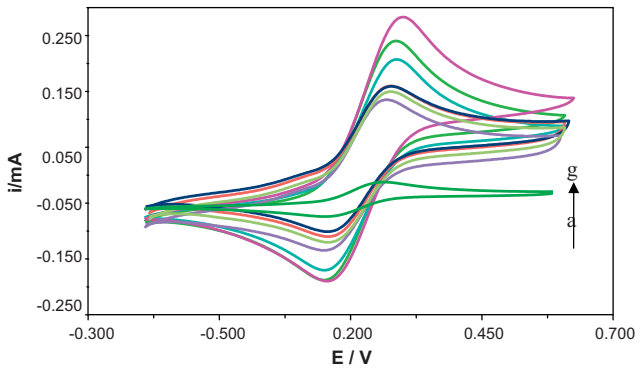

Fig. 3. Cyclic voltammograms recorded at different concentrations of sulfite from (a) 0.5, (b) 100, (c) 200, (d) 400, (e) 600, (f) 800 and (g) 1000 μM, scan rate 50 mV s^{-1}.

sulfite in 0.1 M Tris–HCl buffer solution (pH 8.5) was also investigated. A potential scan rate of 50 mV s^{-1} was selected, since with these experimental conditions, the highest analytical signal and very good cyclic voltammogram profiles were obtained. The optimum response of the present electrode was observed within 2 s. The response of the present electrode system in relation to the change in sodium sulfite concentration was found linear in the range of 0.50–1000 μM (Fig. 3). The Lineweaver–Burk plot between 1/I (μA) and 1/[sulfite] yielded a K_m (apparent) of 8 μM and I_{max} 52.63 μA.

3.8. Evaluation of the performance of the biosensor

3.8.1. Linearity

There was a linear relationship between current (μA) and sulfite concentration ranging from 0.50 to 10 μM (lower concentration range) with linear equation being $y = 3.1402x + 2.2104$ and 100–1000 μM (higher concentration range) with linear equation being $y = 0.3612x + 6.1928$ (Fig. 4), which was better than earlier biosensors based on SO_X immobilized onto polyaniline-sulfonic acid (1–60 μM) (Spricigo et al., 2009), polytyramine-platinized glassy carbon electrode (2–300 μM) (Situmorang et al; 1999), SO_X/AuNP's/CHIT/cMWCNT/PANI/Au electrode (0.75–400 μM) (Rawal et al., 2011).

3.8.2. Detection limit

The detection limit of the present sensor was 0.15 μM (S/N = 3), which is lower than that for enzyme immobilized onto SO_X/AuNP's/CHIT/cMWCNT/PANI/Au electrode (0.5 μM) (Rawal et al., 2011), polypyrrole films (0.9 μM) (Ameer and Adeloju, 2008), polyaniline-sulfonic acid (1 μM) (Spricigo et al., 2009), polytyramine-platinized glassy carbon electrode (2 μM) (Situmorang et al., 1999), and Teflon membrane (200 μM) (Sezginturk and Dinckaya, 2005).

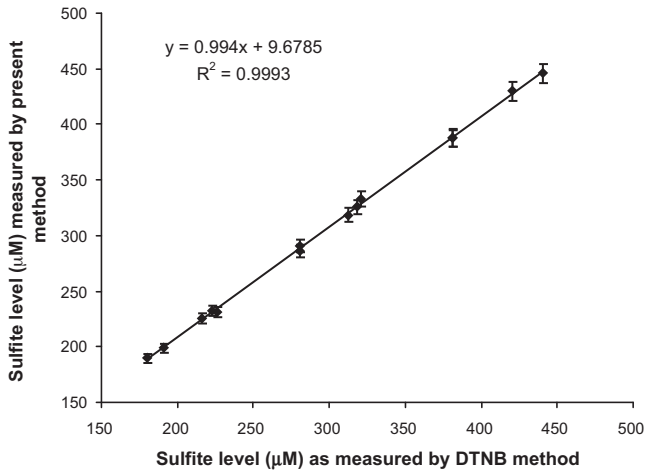

Fig. 5. Correlation between sulfite values as determined by standard DTNB method (*x*-axis) and present biosensor method employing SO_X/Fe_3O_4@GNPs/Au electrode (*y*-axis). Error bars represent the standard deviation for three independent measurements.

3.8.3. Recovery and precision

The analytical recoveries of added sulfite in red wine (50 μM and 100 μM) were 95.40% to 96.46% respectively, demonstrating the satisfactory accuracy of the present method. Within and between coefficients of variation were 1.7% and 3.3% respectively. The high precision indicated the good reproducibility and consistency of the present method.

3.8.4. Correlation

A comparison of sulfite values in 15 brands of red wines as measured by the present method (*y*) with those obtained by standard DTNB method (*x*) showed a good correlation with $r = 0.96$, regression equation being, $y = 0.994x + 9.6785$ (Fig. 5). These results indicate the high accuracy of the method.

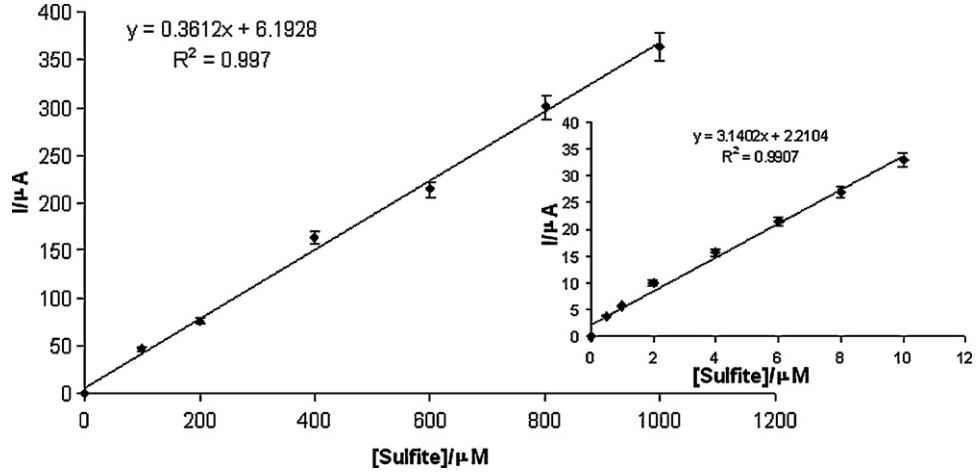

Fig. 4. The calibration curve for sulfite biosensor. *Inset*: Calibration curve at a concentration below 10 μM sulfite. Error bars represent the standard deviation for three independent measurements.

3.9. Interference study

The addition of the following interferrants such as ascorbic acid (4.8 μM), cysteine (0.24 μM), fructose (60 μM), glucose (22.2 μM), citric acid (100 μM), ethanol (70 μM) and glutamine (85 μM) evoked a negligible interference (a decrease of only 6.44% for glutamine, 3.76% for glucose, 6.63% for citrate, 3.99% for fructose, 4.13% for cysteine and 7.66% for ascorbic acid on the biosensor response).

3.10. Storage stability and reusability of biosensor

The electrode lost 30% of its initial activity after its 300 uses during the span of 4 months when stored at 4 °C, which is much better than earlier biosensors (Abass et al., 2000; Spricigo et al., 2009; Rawal et al., 2011).

3.11. Application of sulfite biosensor for determination of sulfite in red and white wines

Sulfite level as measured by the present biosensor ranged from 180.5 to 440.4 μM in red wines and 383–780.6 μM in white wines (Supplementary Table 1) which is comparable to earlier report (Isaac Livingstone et al., 2006).

4. Conclusion

The use of modified SO_X/Fe_3O_4@GNPs/Au electrode has resulted into an improved analytical performance of the sulfite biosensor in terms of low response time (2 s), lower/better detection limit, 0.15 μM (S/N = 3), higher storage stability (120 days), wider linear range (0.5–1000) and no interference by various interferrants compared to earlier biosensors. Based on these results, this composite could also be exploited for the improvement of analytical performance of other biosensors.

Appendix A. Supplementary data

Supplementary data associated with this article can be found, in the online version, at doi:10.1016/j.bios.2011.10.007.

References

Abass, A.K., Hart, J.P., Cowell, D., 2000. Sens. Actuators B 62, 148–153.
Ahmad, A., Sarfraz, A., 2010. Indian J. Exp. Biol. 48, 83–86.
Ameer, Q., Adeloju, S.B., 2008. Electroanalysis 20, 2549–2556.
Bahmani, B., Moztarzadeh, F., Mohammad, R., Mohammadreza, T., 2010. Synth. Met. 60, 2653–2657.
Bias, R., Potezny, N., Edward, J.B., Rofe, A.M., Conyer, R., 1980. Anal. Chem. 52, 508–511.
Bodker, S., Morup, Linderoth, S., 1994. Phys. Rev. Lett. 72, 282–285.
Cho, S.J., Idrobo, J.C., Olamit, J., Liu, K., Browning, N.D., Kauzlarich, S.M., 2005. Chem. Mater. 17, 3181–3186.
Daniel, M.C., Astruc, D., 2004. Chem. Rev. 104, 293–346.
Dinckaya, E., Sezginiturk, M.K., Akyilmaz, E., Ertas, F.N., 2007. Food Chem. 101, 1540–1544.
Isaac Livingstone, A.C., Wain, A.J., Compton, R.G., Davis, J., 2006. Trends Anal. Chem. 25, 589–598.
Jaffrezic-Renault, N., Martelet, C., Chevolot, Y., Cloarec, J.P., 2007. Sensors 7, 589–614.
Kaeil, R., Hampp, R., Ziegler, H., 1989. Anal. Chem. 61, 1755–1758.
Katz, E., Willner, I., Wang, J., 2004. Electroanal 16, 19–44.
Kuang, H.M., Deng, Z.X., Li, C.H., Sun, X.M., Zhuang, J., Li, Y.D., 2002. Acta Phys. Chim. Sinica 18, 477–480.
Laurent, S., Forge, D., Port, M., 2008. Chem. Rev. 108, 2064–2110.
Li, G., 2007. In: Kumar, C. (Ed.), Nanotechnologies for Life Sciences, Vol. 8. Nanomaterials for Biosensors. Wiley-VCH, pp. 278–310.
Mikhaylova, M., Kim, K.D., Berry, C.C., Zogorodni, A., Toprak, M., Curtis, A.S.G., Muhammed, M., 2004. Chem. Mater. 16, 2344–2354.
Pizzoferrato, L., Quattrucci, E., Di Lullo, G., 1989. In: Walker, R., Quattrucci, E. (Eds.), Nutritional and Toxicological Aspects of Food Processing. Taylor and Francis, London, pp. 93–98.
Rahman, M.M., Umar, A., Sawada, K., 2009. Sens. Actuators B 137, 327–333.
Rawal, R., Chawla, S., Dahiya, T., Pundir, C.S., 2011. Anal. Bioanal. Chem. 401, 2599–2608.
Safavi, A., Ramezani, Z., 1997. Talanta 44, 1225–1230.
Satyapal, Pundir, C.S., 1993. Biochim. Biophys. Acta 1161, 1–6.
Sezginturk, H.K., Dinckaya, E., 2005. Talanta 65, 998–1002.
Situmorang, M., Hibbert, D.B., Gooding, J.J., Barnett, D., 1999. Analyst 124, 1775–1779.
Spricigo, R., Dronov, R., Lisdat Leimkühler, F., Frieder, S., Scheller, W., Wollenberger, U., 2009. Anal. Bioanal. Chem. 393, 225–233.
Stammati, A., Zanetti, C., Pizzoferrato, L., Quattrucci, E., Tranquilli, G.B., 1992. Food Addit. Contam. 9, 551–560.
Mohammad, H., 2008. Iran J. Chem. Chem. Eng. 27, 115–121.
Theisen, S., Hansch, R., Kothe, L., Galensa, R., 2010. Biosens. Bioelectron. 26, 175–181.
Wan, J.Q., Cai, W., Feng, J.T., 2007. J. Mater. Chem. 17, 1188–1192.
Zhu, X., Han, K., Li, G., 2006. Anal. Chem. 78, 2447–2449.
Zhang, D., Zhao, J., Li, G., 2008. Protein Pept. Lett. 15, 764–771.